

Electro-optical switching at 1550 nm using a two-state GeSe phase-change layer

Richard Soref,^{1,*} Joshua Hendrickson,² Haibo Liang,³ Arka Majumdar,⁴ Jianwei Mu,⁵ Xun Li,³ and Wei-Ping Huang⁶

¹*Physics Department and the Engineering Program, University of Massachusetts at Boston, Boston, Massachusetts 02125, USA*

²*Air Force Research Laboratory, Sensors Directorate, Wright-Patterson Air Force Base, Ohio 45433, USA*

³*Department of Electrical and Computer Engineering, McMaster University, 1280 Main Street West, Hamilton, ON L8S 4L8, Canada*

⁴*Department of Electrical Engineering, University of Washington, Seattle, Washington 98195, USA*

⁵*Microphotronics Center and Department of Materials Science and Engineering, Massachusetts Institute of Technology, Cambridge, Massachusetts 02139, USA*

⁶*School of Information Science and Engineering, Shandong University, 27 Shanda Nanlu, Jinan, Shandong 250100, China*

*soref@rcn.com

Abstract: New designs for electro-optical free-space and waveguided 2 x 2 switches are presented and analyzed at the 1.55 μm telecoms wavelength. The proposed devices employ a ~10 nm film of GeSe that is electrically actuated to transition the layer forth-and-back from the amorphous to the crystal phase, yielding a switch with two self-sustaining states. This phase change material was selected for its very low absorption loss at the operation wavelength, along with its electro-refraction $\Delta n \sim 0.6$. All switches are cascadeable into N x M devices. The free-space prism-shaped structures use III-V prism material to match the GeSe crystal index. The Si/GeSe/Si “active waveguides” are quite suitable for directional-coupler switches as well as Mach-Zehnder devices—all of which have an active length 16x less than that in the free-carrier art.

©2015 Optical Society of America

OCIS codes: (230.2090) Electro-optical devices; (160.2100) Electro-optical materials; (310.2785) Guided-wave applications; (240.3990) Micro-optical devices; (130.4815) Optical switching devices.

References and links

1. J. L. Bosse, I. Grishin, Y. G. Choi, B. K. Cheong, S. Lee, O. V. Kolosov, and B. D. Huey, “Nanosecond switching in GeSe phase change memory films by atomic force microscopy,” *Appl. Phys. Lett.* **104**(5), 053109 (2014), doi:10.1063/1.4863495.
2. H. W. Ahn, D. S. Jeong, B. K. Cheong, H. Lee, H. Lee, S. D. Kim, S. Y. Shin, D. Kim, and S. Lee, “Effect of density of localized states on the ovonic threshold switching characteristics of the amorphous GeSe films,” *Appl. Phys. Lett.* **103**(4), 042908 (2013).
3. G. H. Park, C. S. Hwang, S. Lee, and B. K. Cheong, “Threshold resistive and capacitive switching behavior in binary amorphous GeSe,” *J. Appl. Phys.* **111**(10), 102807 (2012).
4. K. Jarvis, R. W. Carpenter, M. Davis, and K. A. Campbell, “An investigation of amorphous Ge_2Se_3 structure for phase change memory devices using fluctuation electron microscopy,” *J. Appl. Phys.* **106**(8), 083507 (2009).
5. S. Kurinec, A. Devasia, D. Cabrera, S. Raoux, D. MacMahon, and K. A. Campbell, “Stacked chalcogenide layers for phase change memory,” *Proc. European Phase-Change and Ovonics Symposium* (4 Sept. 2011).
6. H. Liang, R. Soref, J. Mu, A. Majumdar, X. Li, and W.-P. Huang, “Simulations of silicon-on-insulator channel-waveguide electro-optical modulators and switches using a $\text{Ge}_2\text{Sb}_2\text{Te}_5$ self-holding layer,” *J. Lightwave Technol.* (to be published).
7. J. Hendrickson, R. Soref, J. Sweet, and A. Majumdar, “Electro-optical 1 x 2, 1 x N and N x N fiber-optic and free-space switching over 1.5 to 3.0 μm using a Ge- $\text{Ge}_2\text{Sb}_2\text{Te}_5$ -Ge prism structure,” *Opt. Express* (to be published).
8. R. A. Soref, “Liquid-crystal fiber-optic switch,” *Opt. Lett.* **4**(5), 155–157 (1979).
9. R. A. Soref, “Electrooptic 4x4 matrix switch for multimode fiber-optic systems,” *Appl. Opt.* **21**(8), 1386–1393 (1982).
10. J. Choi, A. Singh, E. A. Davis, and S. J. Gurman, “Optical properties and structure of unhydrogenated, hydrogenated and zinc-alloyed a- $\text{Ge}_x\text{Se}_{1-x}$ films prepared by radio-frequency sputtering,” *J. Non-Cryst. Solids* **198–200**, 680–683 (1996).

11. R. R. Romanyuk, I. S. Dutsyak, and A. G. Mikolaichuk, "Effect of gamma irradiation on the optical properties of amorphous GeSe films," *Inorg. Mater.* **43**(6), 584–587 (2007).
12. A. M. Elkashy, "Optical constants of Germanium Selenide single crystals in the transparency region," *Phys. Status Solidi B Basic Res.* **149**(2), 747–758 (1988).
13. K. Petkov, G. Vassilev, R. Todorov, J. Tasheva, and V. Vassilev, "Optical properties and structure of thin films from the system $\text{GeSe}_2\text{-Sb}_2\text{Se}_3\text{-AgI}$," *J. Non-Cryst. Solids* **357**(14), 2669–2674 (2011).
14. S. K. Bhadra, A. K. Maiti, and K. Goswami, "Photo-darkening in GeSe film by CW laser irradiation," *J. Mater. Sci. Lett.* **18**(19), 1543–1545 (1999).
15. M. Nedeljkovic, R. Soref, and G. Z. Mashanovich, "Free-carrier electrorefraction and electroabsorption modulation predictions for silicon over the 1 to 14 μm infrared wavelength range," *IEEE Photonics Journal* **3**(6), 1171–1180 (2011).
16. R. Soref, "Mid-infrared 2 \times 2 electro-optical switching by silicon and germanium three-waveguide and four-waveguide directional couplers using free-carrier injection," *Photonics Research* **2**(5), 102–110 (2014).

1. Introduction

The stoichiometric IV-VI compound GeSe has been identified as a phase-change material (PCM) having two stable, self-sustaining states: its amorphous and crystalline phases [1–5]. This PCM has the capability of high-speed reversible transition between phases (occurring in 100 ns or less), and a recent paper [1] reports experiments on electrically actuated transitions using a field of $\sim 80 \text{ V}/\mu\text{m}$ applied to the GeSe film. Using such electrical control, the optical contrast between the two states of GeSe can be exploited in a suitable wavelength range by incorporating a thin GeSe film within the electro-optical structures that are proposed and analyzed in this paper.

Looking at refractive index data given in the literature, we see that a key feature of GeSe is its very low optical absorption loss in both phases at the important wavelength of 1550 nm. We have targeted this C-band wavelength for device exploration because 1550 nm has become an "essential point of operation" in fiber-optic networks as well as silicon photonics. The complex index of GeSe is $n + ik$, and if the subscripts am and cr are used to denote the amorphous and crystalline phases, respectively, then it is clear that the extinction coefficients k_{am} and k_{cr} are less than 10^{-4} at $\lambda = 1550 \text{ nm}$. That fact affords an opportunity to develop specialized low-loss electro-optical (EO) switching components for telecommunication and optical wireless applications.

The basic switching function is 1 \times 2 and 2 \times 2 spatial routing, and these devices are the building blocks that can be cascaded into 1 \times N and N \times N network switches. Recent theoretical design studies at the 2 to 3 μm wavelengths [6,7] show that a two-pronged approach to PCM EO switching can be taken, namely the switching of light traveling within (1) silicon channel waveguides or (2) "prism structures" to which lensed optical fibers are attached. This paper investigates both avenues. The prior work [6,7] dealt with $\text{Ge}_2\text{Sb}_2\text{Te}_5$ that exhibits significant loss at 1550 nm unlike the present GeSe. However, the earlier designs do offer guidelines for the present studies. The results of [6] show that a thin "active" PCM layer buried at midlevel in the semiconductor channel can produce a significant effective-index perturbation in the composite channel due to the strong overlap of the mode with the layer. The EO effect is "large." The result in [7] is that collimated light beams can be "manipulated" by a three-part "macro-scale" dielectric structure in which a thin active PCM layer is sandwiched between a pair of transparent, high-index semiconductor prisms. This "trio" offers dramatic variation of each beam's reflection and transmission by controlling the PCM electrically.

This paper is organized as follows. The objectives of the paper are outlined. Then the complex indexes in two phases of GeSe are discussed, after which prism structures that encapsulate GeSe are proposed and analyzed for the switching of unpolarized light. Finally a new kind of SOI channel waveguide (encapsulating GeSe) is proposed and analyzed as the active region in 2 \times 2 devices. Switching predictions are made.

2. Objectives and significance

Free-space switching and waveguided switching are examined and compared in this paper. Taken together, these two "classes" of switches span a "space of functions" that one would

want an EO switch to perform. Our objective in this paper is to assess the “competence” and the limitations of each class. Regarding capabilities, we look first at the free-space prism structures. Evidence is given in section 4 that 2×2 and 1×4 routing of fiber-optic light will be effective. An additional free-space application that does not involve fibers is the EO spatial light modulator (SLM), a device that presupposes that the GeSe layer is sub-divided into a 2D array of small pixels, each of which is independently controlled electrically by localized electrode structures. Although the SLM appears feasible, a caveat is that the prisms provide $\sim 53^\circ$ incidence upon the GeSe, and this obliqueness may hinder the easy insertion of the SLM into the system optics. A third free-space switching function is optical beam steering, or more accurately, beam displacement; for example, the four-position side movement of the beam given by the 1×4 device.

Turning now to the significance of the waveguided devices, the studies detailed below give reason to think that 2×2 waveguided switching will be practical in Mach-Zehnder-interferometer (MZI) and directional-coupler structures, all of which will have a comparatively small “footprint” on the integrated-optic network chip. The small size is a PCM advantage. That compactness is traceable to the large index changes provided by GeSe phase change. As indicated above, the optical interconnection or “cascading” of elemental switches is feasible readily in both the free-space and the guided-wave switches. Thus, in principle, higher-order $N \times M$ switching can be accomplished in both categories. However, here the unanswered question is whether the optical insertion loss and the optical crosstalk will build up to unacceptable levels in an $N \times M$. In the future, this issue needs to be resolved on a case-by-case basis.

One way to gauge the significance of these phase change switches is to place them in the context of other guided-wave switching schemes such as those that rely upon: the depletion or injection of free carriers, the thermo-optic effect, the Franz-Keldysh effect, the quantum-confined Stark effect, and the Pockels effect found in a second-order organic polymer embedded in a silicon waveguide. The relationship between the phase-change technique and these other switching approaches can be described in terms of metrics such as switching speed, holding voltage, energy consumption, voltage levels, insertion loss (IL), optical crosstalk (CT), and the device size mentioned above. Regarding speed, a general point is that a switch often routes packets of information or “messages” instead of handling individual bits as in a digital 1×1 EO modulator, meaning that the speed requirements of switches are often relaxed compared to those of modulators. Having said that, we note that the ~ 100 ns required to recrystallize GeSe from the amorphous phase, and the ~ 10 ns required to melt and quench GeSe into the amorphous phase—the transition times—are longer than the on/off times found in several of the above-listed switching effects—a PCM disadvantage.

Earlier studies of phase change memories [1–5] and latched waveguides [6] reveal that the self-holding behavior of the PCM is a general advantage because all of the alternative switches mandate a holding-on voltage for their second switching state. No sustaining voltage is needed in PCM. Earlier simulations of a waveguided 10-nm waveguide GST film [6] indicate voltage requirements of ~ 5 V for am-to-cr and ~ 15 V for cr-to-am. Those results apply directly to the present GeSe case. For the prism structures in section 4 below, we estimate that those two transition voltages are ~ 10 V and ~ 30 V, respectively. The specific voltage depends upon the GeSe film thickness selected. These PCM transition voltages are generally higher than those utilized in competing switches—a disadvantage. However, the loss and crosstalk of the PCM switch that we have estimated in this paper are competitive with those attained in the alternative switching art where PCMs are not used.

The PCM prism structures in section 4 are based directly upon early *experimental* prism structures [8,9] in which the active layer was a thin film of voltage-controlled, oriented nematic liquid crystal (LC). This early foundation is significant because it gives us confidence that the PCM switch can be engineered in a practical sense. An advantage here is that the PCM offers much shorter response times than the \sim millisecond rise and fall times of the LC switch.

3. GeSe indexes of refraction at 1550 nm

The optical bandgap of rf-sputtered amorphous GeSe has been reported as ~1.5 eV [10] and as 1.25 eV for a flash-evaporated layer [11] while the crystal-phase bandgap is 1.08 eV [12]. The real index of the GeSe orthorhombic crystal phase is reported in the experimental measurements of Elkashy *et al* on cleaved single crystals [12] as being $n_{cr} = 2.91$ for light polarized along the a-axis, while $n_{cr} = 2.97$ for the c-axis polarization. We shall make the approximation in this paper that $n_{cr} = 2.97$ for both polarizations. Nano-crystallization in a thin film might yield different values. The real index of the GeSe amorphous phase depends to some extent upon (1) the technique used for film deposition, (2) the film's thickness, and (3) whether or not the deposited film was annealed. That is why it is difficult to cite a "definitive" value for n_{am} . In the related material GeSe₂ there is however agreement that $n_{am} = 2.36$. For GeSe at 1550 nm, Bhadra *et al* [13] report $n_{am} = 2.2$, whereas [14] reports $n_{am} = 2.5$ at an unspecified wavelength in the transparency region. Lacking additional literature data, and being conservative on $n_{cr} - n_{am}$, we shall assume that $n_{am} = 2.4$. Regarding the aforementioned optical bandgap E_g of the amorphous phase, the "method of preparation" influence could explain or reconcile the different reported E_g values.

As to the 1550-nm extinction coefficients, there is consensus in the literature that both k_{am} and k_{cr} are "nominally zero." However, in practice both of these loss factors do have finite values, and so for the purposes of our device modeling we shall assume the presence of background loss "k" for both phases of GeSe. The literature presents curves of absorption coefficient versus wavelength near the band edge of GeSe and from an extrapolation of those curves we estimate that the background loss α is in the range of 5 cm^{-1} at 1550 nm, the value assumed here, which is ~22 dB/cm. The k value is given by $k = \alpha\lambda/4\pi$, thus we shall take $k_{am} = k_{cr} = 6 \times 10^{-5}$. The doped silicon channel waveguides discussed below in section 4 are assumed to have a localized N-type doping of $1 \times 10^{18} \text{ cm}^{-3}$, and at 1550 nm, the donors are known [13] to induce a loss of 8 cm^{-1} which produces 35 dB attenuation per cm of doped channel. The Si-related background extinction of 10^{-4} is entered below for both switch states. In summary (Table 1):

Table 1. Values of the indices that were utilized in the present simulations

Material	Complex Index
N-Silicon $1 \times 10^{18} \text{ cm}^{-3}$	$3.47 + 0.0001i$
Silicon Dioxide	$1.45 + 0i$
GeSe (state 1) amorphous	$2.4 + 0.00006i$
GeSe (state 2) crystal	$2.97 + 0.00006i$

4. Prism structures for EO switching

The Hendrickson *et al* paper [7] describes how a thin film of PCM is sandwiched between two semiconductor prisms to provide grazing-incidence optical coupling of collimated infrared beams to the film. For the two-prism EO device, two light beams are incident upon the device. Each beam has the same angle of incidence upon the PCM. Within the volume of each "overlapped" prism, a thin highly doped region is in contact with the PCM (see Fig. 2 of [7]). This provides two external contacts for an external voltage source that will trigger the desired phase transition. The local thin doping does not introduce significant optical loss. Our proposed 2 x 2 switch is illustrated in Fig. 1 for infrared beams and optical fibers, respectively. The isotropic index of each semiconductor prism is denoted as n_s , and the strategy adopted in [7] was to select n_s so that $n_s = n_{am}$. That strategy was to some extent "forced" by the $n_{am} \sim 4.0$ of the prior PCMs. There, the possibility of matching n_s to the prior $n_{cr} \sim 6.8$ was ruled out. Certainly, the $n_s = n_{am}$ strategy can be utilized here in the case of GeSe film. However, instead of that, a better strategy opens up now because the GeSe index values are low by comparison to those of GeTe and Ge₂Sb₂Te₅.

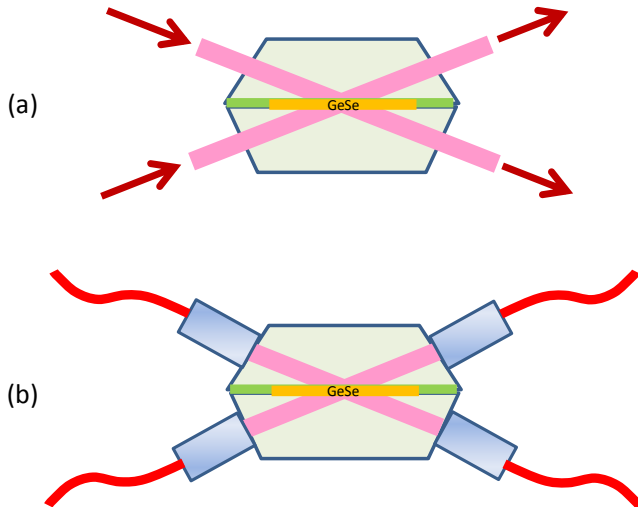


Fig. 1. Cross-section side view of proposed 1550-nm EO 2 x 2 prism-structures using switchable-TIR GeSe thin film for (a) collimated light beams, (b) optical lensed-fibers.

In this paper, we propose a new strategy for switching both the S- and P- polarization of incoming light (polarizations denoted henceforth as TE and TM, respectively). The idea is to approximately match the prism index n_s to the crystal index n_{cr} . The best-case scenario is when n_s is *slightly larger* than n_{cr} . This technique works well when n_s is at least 20% larger than n_{am} which applies here. Classical optics tells us what happens. The PCM film has states 1 and 2 corresponding to n_{am} and n_{cr} . The 1550-nm beam enters the n_s prism (the “dense medium”) where it then impinges upon the “less dense” (lower index) GeSe medium. The TM experiences Brewster angle behavior, while TE does not. However, both TE and TM in state 1 experience total internal reflection (TIR) for an incidence angle θ that is greater than the critical angle $\theta_{c1} = \text{arc sin}(n_s/n_{am})$. Similarly, both TE and TM have TIR when $\theta > \theta_{c2} = \text{arc sin}(n_s/n_{cr})$. The trick is to choose $\theta_{c1} < \theta \leq \theta_{c2}$ so as to have total transmission in state 2. That approach ensures strong switching of un-polarized light for which the input beam has both TE and TM components. To give a concrete example, assume that the prisms are made from crystalline GaP whose index is 3.06 at 1550 nm. (In addition, there are III-V alloys whose index comes closer to 2.96). Then we find $\theta_{c1} = 51.7^\circ$ and $\theta_{c2} = 75.3^\circ$. As mentioned, our proposal is to select an incidence angle between θ_{c1} and θ_{c2} such as $\theta = 53^\circ$. This is quantified below.

TE and TM are both switched in each state, where state 1 has very high un-polarized reflection, and state 2 has very high un-polarized transmission; thus this is a true 2 x 2 switch. Figure 2 and Fig. 3 present simulation results for the Fig. 1 GaP/GeSe/GaP switch for various choices of GeSe film thickness in the 10 to 100 nm range. Here we used a three-layer Fabry-Perot calculation [7] that took into account dielectric loss in the film as well as thin-film interference effects. The results show that there is freedom in the choice of GeSe thickness. The metrics for switching are the insertion loss (IL) and crosstalk (CT) in each state. It is interesting and beneficial that the TE component of reflection stays very low for $\theta < \theta_{c2}$: lower CT than in the thick-film case. The IL and CT metrics in Figs. 2 and 3 are quite favorable in both states 1 and 2 with θ chosen anywhere in the 53° to 70° range, although $\theta = 53^\circ$ is clearly the most practical choice. Table 2 presents the result of our simulation.

Table 2. Fractional transmission and reflection of a collimated 1550-nm light beam incident at 530 upon a 50-nm GeSe film in the GaP/GeSe/GaP EO 2 x 2 switch with $k = 0.00006$

Mode pol.	State 1 Trans.	State 1 Refl.	State 2 Trans.	State 2 Refl.
TE	0.005	0.987	0.9997	0.024
TM	0.012	0.979	0.9999	0.002

The higher-order 1 x N and N x N switches have been described in [7] and [9] for $\text{Ge}_2\text{Sb}_2\text{Te}_5$ and LCs, respectively, and those device geometries apply here immediately to the GeSe case. Going into more detail, we are now proposing a 1 x N switch that goes beyond the TE-polarized 1 x N of [9] because here we can route unpolarized light. This is illustrated in Fig. 4 in which we use TIR at the GaP/air interfaces to transfer a locally unswitched infrared beam to the next locally active GeSe area (each of four areas has independent electrical addressing as in [7,9]).

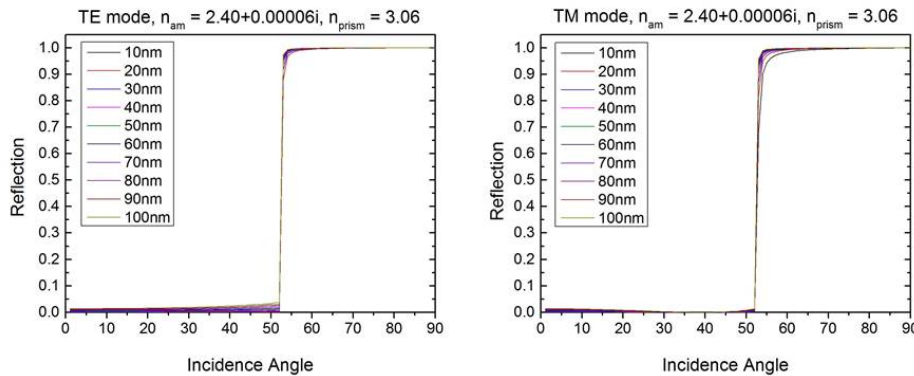


Fig. 2. Amorphous-phase switching of TE and TM light by the GaP/GeSe/GaP prism structure. The 1550-nm incidence angle will be greater than the TIR angle shown.

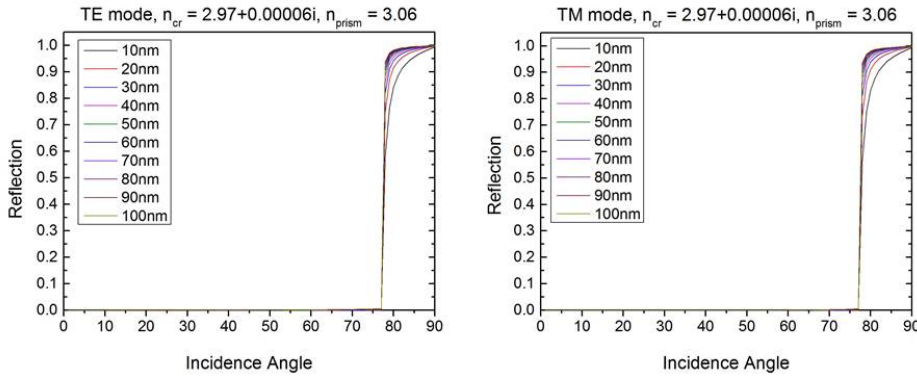


Fig. 3. Crystal-phase switching of TE and TM light by the GaP/GeSe/GaP prism structure. The 1550 nm incidence angle will be less than the TIR angle shown.

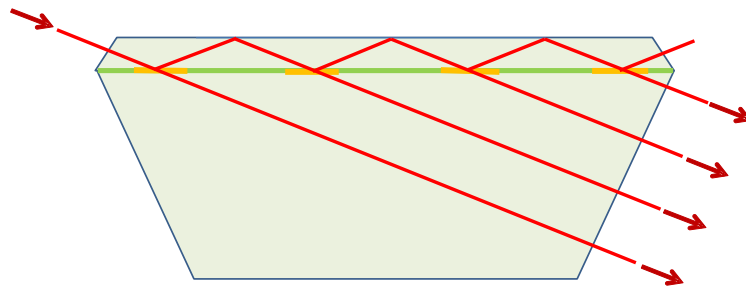


Fig. 4. Cross-section side view of proposed 1×4 EO GeSe switch for complete switching of unpolarized 1550 nm light.

5. Silicon-on-insulator channel-waveguide 2×2 EO switches

The second category of switches is SOI channel waveguided devices. In the silicon photonics industry, the most familiar waveguides are single-mode strip-type waveguides having cross-section dimensions of 500 nm x 250 nm at $\lambda = 1550$ nm, with the Si being etched down to the buried oxide. In the present work, our proposal is to form a very thin, horizontal “photonic slot” in the Si strip by inserting at the midline of the channel a film of GeSe whose thickness is of order 10 nm. Here, we are going to dope the upper and lower halves of the Si channel in order to provide electrical contact to both surfaces of the GeSe layer so as to pulse the GeSe with voltage for phase transition. This N doping introduces a small optical loss of 8 cm^{-1} into the Si channel regions [15]. A perspective view of this proposed active EO region, continuously or smoothly end-coupled to passive Si strip channels is illustrated in Fig. 5 with cross-section insets. This waveguide is essentially identical to the one investigated by Liang *et al* [6] for $\text{Ge}_2\text{Sb}_2\text{Te}_5$.

At this point, we identify two categories of 2×2 switches that can readily employ an “active segment” of the Fig. 5 channel in order to achieve “cross-bar” switching of polarized light, either TE_0 or TM_0 . These switches are the Mach-Zehnder interferometer (MZI) and the directional coupler. As Soref has pointed out recently [16], the directional coupler can employ two or three or four channel waveguides arranged in parallel, waveguides that are evanescent-wave side-coupled to each other. We shall denote those EO directional-coupler waveguide switches as 2W, 3W and 4W, respectively.

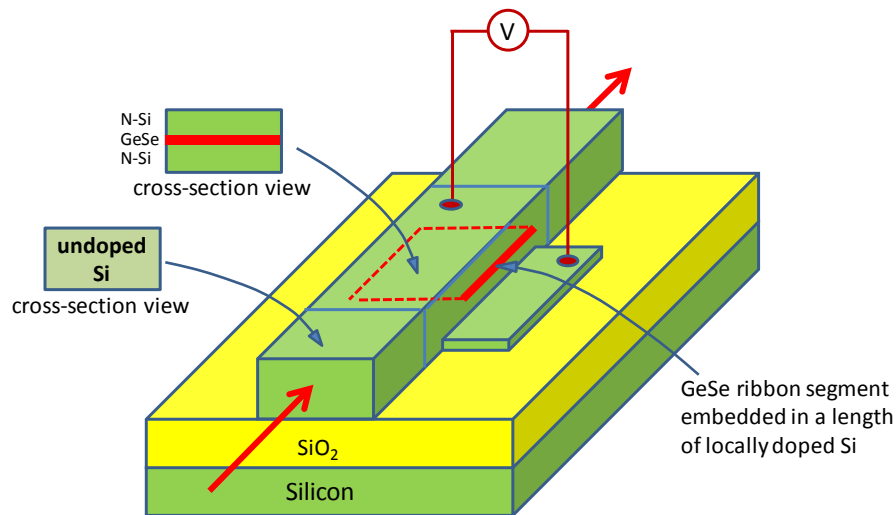


Fig. 5. Smoothly end-coupled SOI active waveguide “segment” utilized in several EO switching devices.

Looking at the typical operating conditions of the MZI and the 2,3,4W's, we see that each device is configured to give the “perfect cross state” in the initial condition of the EO medium. In other words, we are going to arrange a cross state for the amorphous condition of the GeSe film. The goal for “total switching” is to reach the “perfect bar state” of the 2×2 when the GeSe layer is changed into the crystal phase. The work of [16] shows that electro-refraction, a change in the real effective index of the waveguide, is required to reach the bar state. If we write Δn as the voltage-induced change in effective index of the fundamental mode (TE or TM), then the active segment of EO waveguide within the switch (whose length is L) will produce a phase retardation in the mode $\Delta\phi$, where this phase shift is given by $\Delta\phi = \Delta\beta L = (2\pi/\lambda)L\Delta n$. As mentioned earlier for the prisms, there will be a very small background loss in the waveguide at 1550 nm. For the case of the MZI, it is well known in the photonics art that $\Delta\beta L$ of π radians is needed for total switching. For the couplers, the switching requirements have been quantified in detail [16] for the case of weak coupling between waveguides. The results are that $\Delta\beta L$ of 2π is required for 2W, whereas 6π is required for 3W and 4W. Taking $\Delta k \ll \Delta n$, the IL at 6π is 0.3 dB for 3W and is 0.1 dB for 4W. We shall apply those results to the present GeSe waveguides by determining $\Delta\beta$ and L in turn. Our first simulation task is to find the effective indexes for the active Fig. 5 waveguide segment. We assume that a SiO_2 overcoating has been deposited, which means SiO_2 cladding all around the channel. Our first simulations assumed a 10-nm GeSe layer. After that, we examined a 20-nm layer and quickly found that the change in real index was twice as large as that for the 10-nm case. We also compared the effect of increasing the cross-section size $W \times H$ by 25%. It was seen immediately that the 620 nm \times 310 nm channels had much better TM mode confinement in the Si core area. Figures 6 and 7 present the results of mode-profile and effective-index simulations attained using the COMSOL™ wave-module software in the 20-nm GeSe case for both $W \times H$ selections. In these two figures, the optical mode E-field strength is shown in false color represented by the color scale shown at the right in each figure where red denotes the strongest field strength. At the top of each mode profile in Figs. 6 and 7, the calculated value of the complex effective index ($N_{\text{eff}} = n + ik$) is presented for the phase

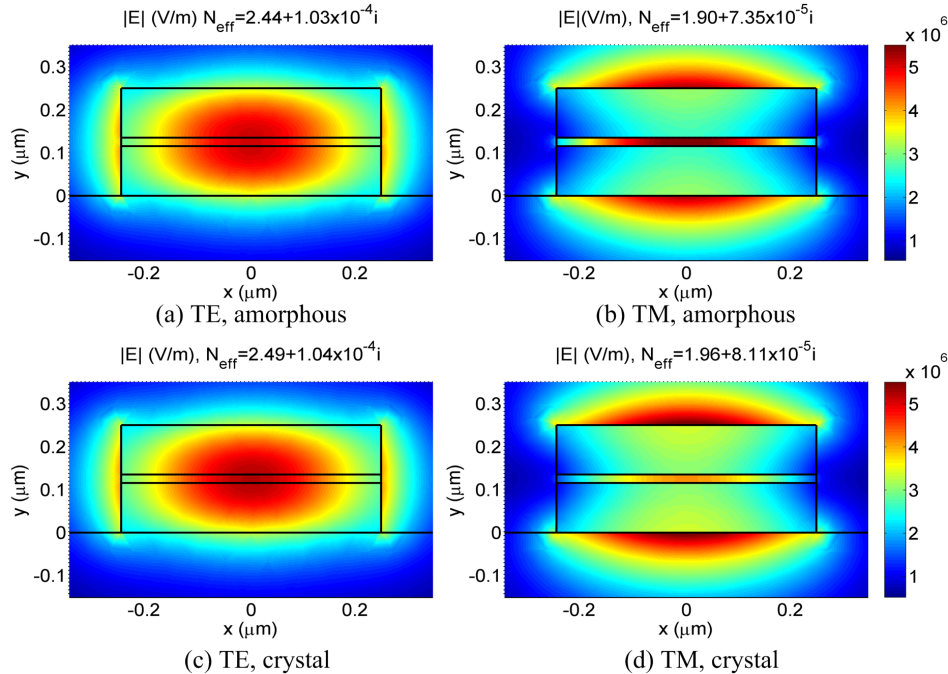


Fig. 6. Mode profile and effective indexes of the N-Si/GeSe/N-Si, 500 nm \times 250 nm waveguide in each state.

of GeSe being studied. By subtracting the N_{eff} found in Fig. 6(a) from that determined in Fig. 6(c), we obtain the change in real effective index Δn along with $\Delta\beta$ and the Δk electroabsorption. A similar $\Delta\beta$ determination is attained by a N_{eff} subtraction between Figs. 6(b) and 6(d); 7(a) and 7(c); 7(b) and 7(d).

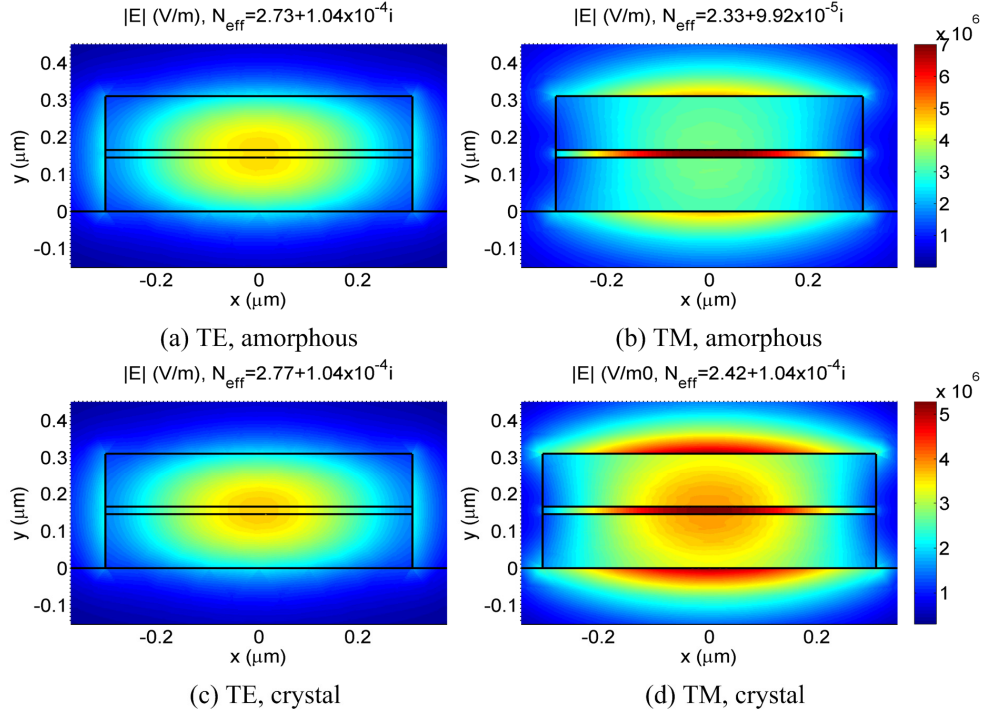


Fig. 7. Mode profile and effective indexes of the N-Si/GeSe/N-Si 620 nm x 310 nm waveguide in each state

Having found Δn and $\Delta\beta$ in Figs. 6 and 7, we referred to the aforementioned $\Delta\beta L$ requirements [16] for four 2 x 2 structures and thereby determined the active length L required to reach the bar state. These EO switching lengths are now tabulated in Table 3.

Table 3. Simulation results on waveguided Si/GeSe/Si 2 x 2 EO switches

Mode	W Nm	H nm	$\Delta\beta$ $(\mu\text{m})^{-1}$	MZI $L(\pi)$ μm	2W DC $L(2\pi)$ μm	3,4W DC $L(6\pi)$ μm
TE	500	250	0.195	16.1	32.2	96.7
TM	500	250	0.252	12.5	24.9	74.8
TE	620	310	0.164	19.1	38.2	114.6
TM	620	310	0.343	9.2	18.3	55.0

The projected L range in Table 3 of 9 to 16 μm for the MZI means that this 2 x 2 will have a very small footprint, certainly much shorter than L in the free-carrier actuated switch where L_{fc} (MZI, π) is about 300 μm . Similarly, the L values predicted here for all three coupler-switches are significantly smaller than those cited in [16]. There is a small IL associated with the background loss. For example, in the worst case of $L = 114.6 \mu\text{m}$ with 40 dB/cm effective background attenuation, then $IL = 0.46 \text{ dB}$. Generally, Table 3 projects improvements in the photonic art.

6. Discussion of waveguided results

It is seen in Figs. 6 and 7 that the TE mode confinement is always better than the TM confinement and that the TM has a noticeable fraction of its energy traveling in the SiO_2 cladding. (Since the cladding is lossless, the considerable TM mode “tailing” does not

produce added propagation loss). The TM mode exhibits photonic slot behavior, especially in the amorphous state, but the TE mode does not show slotting. The waveguides with larger cross section, for both TE and TM, have mode confinement superior to confinement found in the smaller cross section case. The waveguide background loss was about 25 dB per cm of active length in state 1 and was 36 dB/cm in state 2. If we look at the mode profiles of Figs. 6 and 7, the choice of TE versus TM hinges upon whether it is acceptable to use a mode that fringes outside of the core region. The TE is always very well confined in the core and the use of TE entails only a small penalty in its reduced Δn .

We see compactness in the MZI and the couplers. Considering the three coupler switches as a whole, the L range of 17 to 114 μm implies that strong coupling is taking place between adjacent waveguides in order to have the initial cross state produced in a coupling length L_c that is equal to L. Intuitively, the required strong coupling is achievable by narrowing the SiO_2 gaps between parallel channels. However, because the Table 3 $\Delta\beta L$ requirements for 2,3,4W were derived for the weak coupling case, the question still remains as to whether these same $\Delta\beta L$ will induce the perfect bar state in the strong coupling case. This question could be answered via 2D and 3D simulations. But even in the absence of such simulations, a perspective can be given. For example, if the needed $\Delta\beta L$ for the strong case were twice those of the weak case, that would imply simply a doubling of the L's in Table 3, and such lengths are still much more compact than in the weak-coupling art. As mentioned above, for all four 2 x 2 devices, the switch "holds itself" in either state.

5. Conclusion

The C-band wavelength of 1550 nm is quite important in fiber-optic networks and in the associated SOI optoelectronic signal processing chips. Three physical properties of the "emerging" phase-change material GeSe -make it an excellent candidate for exploitation at 1550 nm: (1) a voltage applied to a thin film of GeSe ($E \sim 80\text{V}/\mu\text{m}$) can induce a fast, reversible phase transition between the amorphous and crystal phases, and each phase is self-sustaining without voltage, (2) the optical absorption loss in each phase is less than 40 dB per cm of "active length", and (3) the real refractive index of the crystal phase is about 0.6 larger than that of the amorphous phase. We show specifically how to apply these properties to practical electro-optical device structures. We have proposed and analyzed two techniques for electrically controlled spatial routing of 1550 nm light beams in 2 x 2, 1 x N and N x N geometries, and these devices are capable in principle of switching un-polarized light beams. Both methods employ a 10 to 100 nm film of GeSe. The first is the use of two "macroscopic" doped-semiconductor prisms to provide oblique incidence of "beams" on the film for switchable TIR. The second technique is to sandwich the film at the mid-plane of an SOI channel waveguide to provide a strong electro-refraction effect for light propagating on-axis. This three-layer waveguide constitutes an "active segment" and the active length can couple smoothly at its input and output to a uniform strip of Si channel waveguide. For both methods, transition speeds (reconfiguration times) are in the 100-ns range.

For the prism structure, the prism index is matched to the GeSe crystal index. Then the Fresnel-related equations of a three-layer oblique Fabry-Perot analysis are employed to determine the transmission and the reflection of combined TE and TM polarizations in both states of the switch. Quite favorable IL and CT are predicted for each state in simple and higher-order EO switches.

For the Si/GeSe/Si waveguide structure, films in the 10 to 20 nm range are investigated for waveguide cross-sections W x H of 500 nm x 250 nm and 620 nm x 310 nm, with TEo and TMo being studied. Using COMSOLTM simulations, an effective index determination was made for each case in states 1 and 2, yielding a background loss of ~ 0.004 dB per μm of active length, and an effective electro-refraction Δn around 0.05. We have then applied those findings to a group of 2 x 2 switch structures, the MZI and three directional coupler EO devices—couplers that utilize either two or three or four side-coupled channel waveguides. Our results predict active lengths L for complete switching that are "very short" in the

photonic art, unprecedented in compactness. For the MZI as well as the 2,3,4W, we have highlighted a pathway towards highly integrated, self-sustaining, switching networks.

Acknowledgments

Richard Soref is supported by the Air Force Office of Scientific Research (AFOSR) grant FA9550-14-1-0196 (Gernot Pomrenke, Program Manager) and by the UK EPSRC project MIGRATION. Joshua Hendrickson acknowledges support from AFOSR under LRIR No. 12RY05COR (Gernot Pomrenke, Program Manager). Haibo Liang is financially supported by Natural Sciences and Engineering Research Council of Canada (NSERC) under the Silicon Electronic-Photonic Integrated Circuits (Si-EPIC) CREATE program.